RSS Gradient-Assisted Frontier Exploration and Radio Source Localization

Jeffrey N. Twigg, Jonathan Fink, Paul L. Yu, Brian M. Sadler

***Abstract*— We consider the combined problem of frontier exploration in a complex environment while seeking a radio source. To do this in an efficient manner, we incorporate radio signal strength (RSS) information into the exploration algorithm by locally sampling the RSS and estimating the 2-D RSS gradient. The algorithm adapts the local motion to collect RSS samples for gradient estimation and seeks to explore in a way that brings the robot to the signal source in an efficient manner, avoiding random or exhaustive exploration. An indoor experiment demonstrates the exploration algorithm that uses this information to dynamically prioritize candidate frontiers and traverse to a radio source. Simulations, including radio propagation modeling with a ray-tracing algorithm, enable study of control algorithm tradeoffs and statistical performance.**

I. INTRODUCTION

We consider the combined problem of frontier exploration in a complex environment while seeking a radio source. To do this in an efficient manner, we incorporate radio signal strength (RSS) information into the exploration algorithm by locally sampling the RSS and estimating the RSS gradient. With sufficient average signal-to-noise ratio (SNR) at the receiver, the RSS gradient will provide information about the source direction and the magnitude of the RSS gradient will increase as the range to the source decreases. We demonstrate an exploration algorithm that uses this information to dynamically prioritize candidate frontiers and traverse to the radio source.

Radio connectivity in a complex environment is severely challenged by the rapid fading fluctuation induced by multipath propagation, resulting in dramatic RSS change with relatively small movements [1]. Mobility can be exploited to improve RSS and therefore enhance connectivity in networked teams [2]. The radio propagation environment can be characterized using fading models [3], although a complex environment results in significant spatial variation in the fading model parameters. A nonparameteric approach for RSS mapping using Gaussian processes is given by Fink, et al., where mobile agents learn the environment with a fixed radio source [4]. Here we assume a complex environment creates substantial small scale fading, but we study exploration of a new environment and so do not assume a propagation map is available. We assume the robot the robot can localize itself and can build a map, and that RSS measurements relative to a fixed radio source can only be performed onboard the robot.

In many problems there is a compelling need to maintain communications with other robots or base stations, such as providing sensor information, or maintaining collaborative control. Connectivity may be enhanced by local movement to overcome small scale fading, and with larger movements that generally decrease the propagation distance and enhance average RSS. Local spatial RSS samples can be used to estimate the RSS gradient in two dimensions, providing information about the direction to the source [5], and the RSS gradient can generally be exploited when attempting to localize and navigate to a radio source [6], [7], [5], [8].

In this paper, we advance the ideas of [5] and consider how the 2-D RSS gradient may be used with frontier exploration to robustly guide a robot through an indoor environment to a radio signal source. A frontier is a region which is bordered by explored and unknown space. We assume the robot can sense its immediate environment and determine frontiers available for further autonomous exploration by identifying frontier edge segments [9]. The k-means algorithm is used to identify centers of frontier points. The robot then dynamically selects the next frontier for exploration by incorporating the RSS gradient information as well as the distance to each point. This algorithm incorporates the local motion to collect RSS samples for gradient estimation, and seeks to explore in a way that brings the robot to the signal source in an efficient manner, avoiding random or exhaustive exploration.

II. RSS GRADIENT-ASSISTED EXPLORATION

The goal of the robot is to move to a region with sufficiently high signal-to-noise (SNR) ratio. As the SNR requirement increases, the goal can be interpreted as moving towards and eventually arriving at the signal source. The algorithm described below is outlined in Fig. 1.

To start, the robot has no prior knowledge of the RSS environment, and thus has no directional preference for its movements. Instead, it begins by making RSS measurements as it explores the immediate area. After this initial exploration, it calculates the gradient of the RSS (Appendix I) to determine in which direction the signal strength is increasing the fastest. If the RSS gradient is sufficiently strong, the robot moves in the specified direction to exploit this knowledge; otherwise, the robot continues to explore the local area. In Appendix II, we discuss how to efficiently sample RSS for robust gradient estimates.

After it obtains a preliminary RSS gradient estimate, the robot alternates between *navigation* (selecting the best waypoint from the identified frontiers) and *advancement* (moving towards the current waypoint).

Army Research Laboratory, Adelphi, MD 20783, USA

A. Navigation

The robot identifies candidate frontiers on its map, based on explored and unexplored regions. Next, it ranks these frontiers based on RSS gradient, average RSS, and distance and selects the highest ranking frontier as its waypoint. As the robot moves toward the waypoint, it continually re-evaluates the ranking of the frontiers. Frontiers are re-selected when either (i) the robot reaches original waypoint, or (ii) the ranking of the waypoint drops.

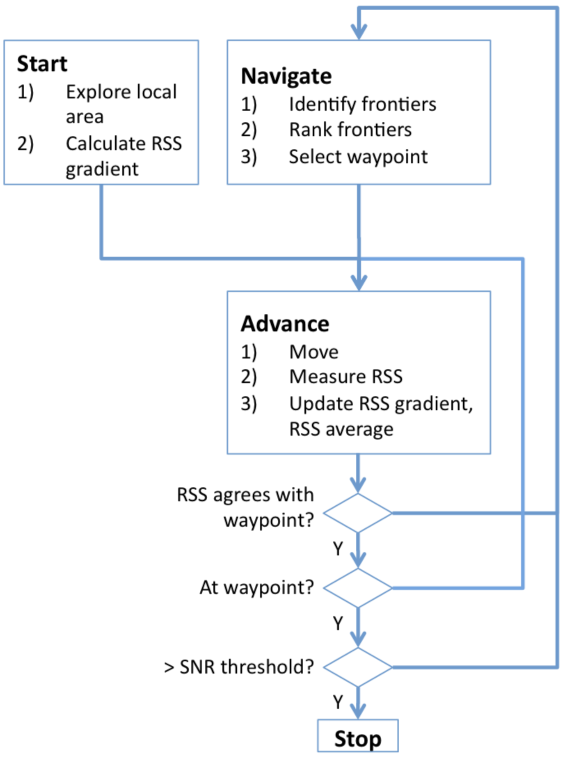

Fig. 1. Flow diagram of the frontier exploration algorithm.

1) Frontier Identification: A frontier is defined by cells in an occupancy-grid map that border known free-space and unknown regions. Frontier segments are identified by a k-means algorithm [10]. This algorithm calculates the centroids of clustered groups based on known boundary cells in the map. We assume that large groups of frontier points correspond to frontier segments that can be pursued during exploration. An example situation is presented in Fig. 2. In this figure, a robot has traversed a subset of the environment. It has cleared an area and identified the known boundary. By clustering with the k-means algorithm, eight frontiers have been identified.

2) Rank Frontiers: Once the set of frontiers is determined, the algorithm ranks them based on three criteria: distance from the current robot position, agreement with RSS gradient, and average RSS magnitude. Fig. 3 depicts an example scenario where these criteria are evaluated.

The distance from the robot's current position to a frontier represents a greedy metric that can be used for exploration. By driving to the closest frontier, unknown space is explored

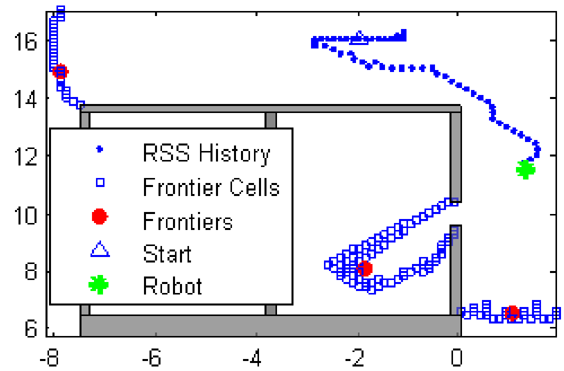

Fig. 2. Illustration of frontier identification for a particular configuration. Points on the boundary of known and unknown space are clustered to identify likely frontiers that can be explored.

with minimum cost. Conversely, this criteria decreases the possibility that a distant frontier is explored without a reasonable expectation to increase the SNR.

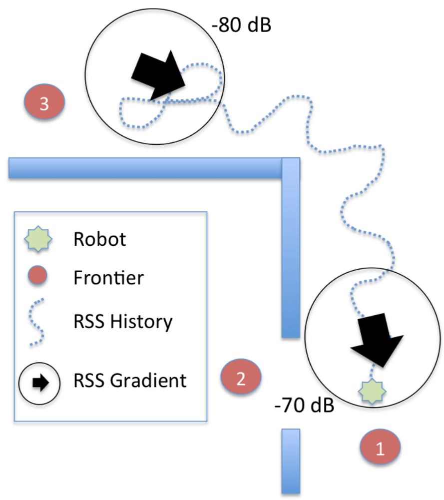

Fig. 3. Example of frontier ranking. Because frontiers 1 and 2 are closely located, they use the same n closest RSS measurements for calculating RSS gradient and average. Frontier 1 is ranked highest because, though distance and RSS are similar to Frontier 2, its direction is closest to the gradient. Frontier 3 is ranked lowest because it is far away, disagrees with the gradient direction, and has the lowest RSS value.

The evaluation of RSS-based metrics requires that a subset of the collected RSS samples be associated with each candidate frontier. This association is computed according to the geodesic or path-distance rather than Euclidean distance such that the n closest samples are associated with each frontier. The RSS gradient and average RSS magnitude is then computed for each subset of RSS samples. When frontiers are far from each other (e.g., at opposite ends of a hallway), the gradient and RSS average tend to be different, and thus lead to easy decisions of which frontier to explore. However, when frontiers are close, the calculations can share many of the same RSS measurements and hence lead to similar results. In this case, though the average RSS magnitude may be very close, the deviation from the gradient information can be used to identify one frontier over the rest.

3) Select waypoint: After computing the above criteria for each candidate frontier, the highest-ranked frontier is chosen as the next waypoint for exploration.

B. Advancement

In typical scenarios, the robot would take the shortest straight-line path to reach the selected frontier. However, this leads to unsuitable RSS gradient estimates because the sampling locations cannot be co-linear, as discussed in Appendix II. Therefore, rather than travel in straight-line trajectories, the robot introduces gentle oscillations to its path (see Fig. 4). This makes the gradient estimate more robust at the cost of greater distance traveled.

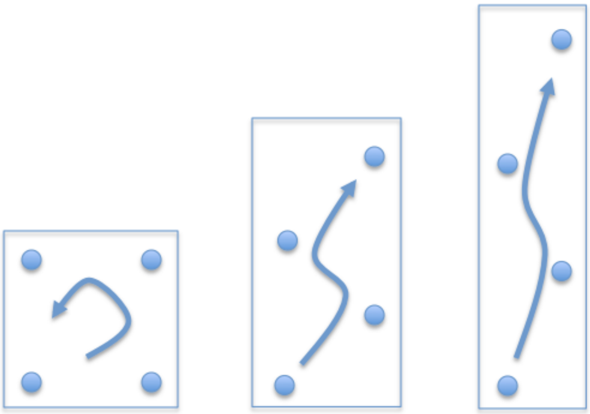

Fig. 4. Moving left to right, the sampling strategies yield more RSS gradient confidence in the vertical direction at the expense of lower confidence in the horizontal direction. In each case, the distance between sampling locations is identical.

As the robot moves towards the current waypoint, it periodically updates its ranking of the set of frontiers based on newly acquired RSS samples. Because it is approaching the waypoint, it collects more accurate gradient data about that particular frontier. When the new RSS measurement corroborate the choice of waypoint (e.g., gradient points towards waypoint, RSS average continues to increase), the robot will continue to the waypoint. Upon reaching the waypoint, if the SNR condition indicating sufficient proximity to the source has not been met, the robot will resume frontier exploration by identifying new frontiers from its current position.

If, in the course of movement towards a waypoint, the gradient becomes contradictory and/or the RSS drops, the robot is able to halt progress before reaching the waypoint and resume frontier exploration by identifying new frontiers from its current position. This capability is particularly useful to avoid exploring large rooms where exploration time can be significant. In order to avoid too many false alarms, we do not halt movement until the current waypoint drops a certain number of ranks in the overall list of candidate frontiers.

III. Experiment and Results

The robot used in the experiments are shown in Fig. 5. The *Scarab* is a small indoor ground platform equipped with a differential drive system, onboard computation, and $802.11a$ wireless communication in addition to its *Zigbee* radio which is used for experimental measurements. It is also equipped with a scanning laser range finder which is leveraged to yield accurate self-localization.

Fig. 5. *Scarab* robot used in experiments. It is capable of self-localization and point-to-point radio signal strength measurements with an off-the-shelf *Zigbee* radio.

The robot has ability to record the RSSI (RSS indicator) reported by the *Zigbee* radio whenever it receives a packet from the fixed source. To smooth the effects of channel noise, the robot averages the RSSI at locations within distance d of each other. We chose d = 12.5cm = 1λ at 2.4 GHz, a distance that has been experimentally shown to result in approximately decorrelated signals [11]. Other testing parameters are shown in Table I.

TABLE I
TABLE OF PARAMETERS

Parameter	Value
number of frontiers (k)	12
number of points to average (n)	10
exploration radius	2.5 m
oscillation amplitude	0.375 m
independent sampling distance	0.125 m

Experimental implementation leads to some modifications to the algorithm described above. To mitigate the limitation that the *Scarab* cannot autonomously identify safe vs. unsafe regions of the environment, we assume an a priori map by which it navigates. The number of possible frontiers was set at $k = 12$ because frontiers would inevitably be identified in unsafe regions that could not be explored. The large number of frontiers help ensure the robot will be able to consider all frontiers as well as ones the robot is not capable of exploring.

In this trial, the *Scarab* starts at one end of the hallway. It randomly explores the local area until it makes a reliable RSS gradient estimate and is able to intelligently select a frontier for exploration. As it oscillates about a path between frontiers, the robot collects RSSI points. However, there are some areas where the robot is not able to receive a signal. In this particular experiment the robot starts exploring away

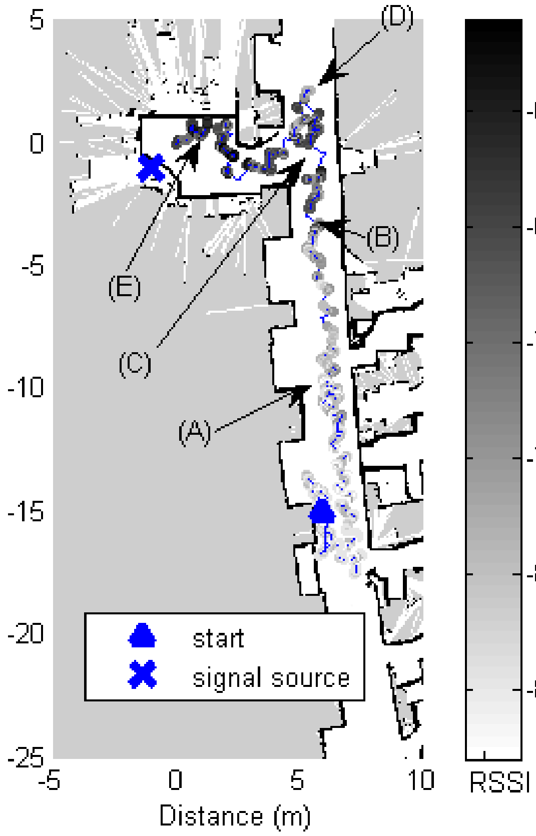

Fig. 6. Trajectory taken in an experimental trial with the *Scarab* mobile robot. Received signal strength at each point is indicated by the intensity. Physical locations (A)–(E) correspond to the points labeled in Fig. 7

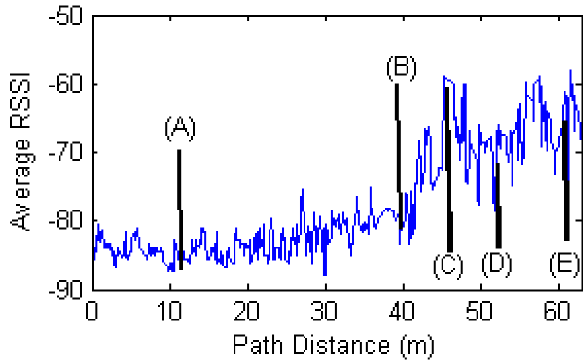

Fig. 7. Received signal strength during the experimental trial depicted in Fig 6. Note that RSS is variable over small distances but generally increases throughout the trial.

IV. Simulation and Results

We also explore aspects of the proposed RSS gradient tracking algorithm through the use of the EMCUBE ray-tracer [12] over a representative office layout shown in Fig. 8. This simulator provides a realistic model of RSS for an indoor space and allows for many tests of the same environment. This allows us to investigate how specific parameters affect the performance of the algorithm.

The simulated signal source transmits at 2.4 GHz. Because we are considering a fixed signal source, RSS is calculated off-line for each point on a grid with wavelength spacing, $\lambda = 12.5$ cm at 2.4 GHz – a distance that has been experimentally shown to result in roughly decorrelated signals [11].

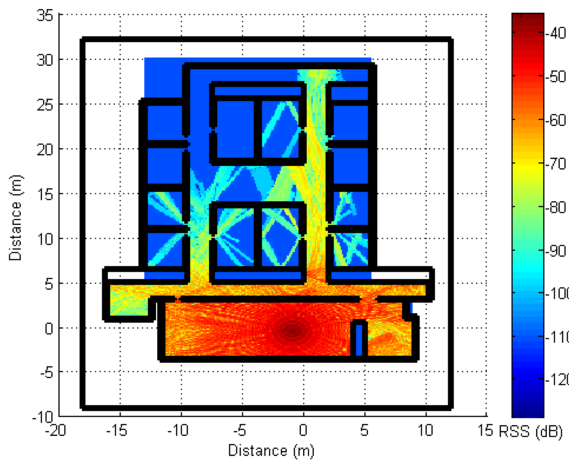

Fig. 8. Map of simulated RSS for a typical indoor environment. Note that the EMCUBE simulation models complex multi-path phenomena

from the source, but turns around after exploring its first frontier. Afterwards it moves up the hallway, past several offices and collects data near the room with the source. The robot detects the higher RSSI average and gradient pointing towards and successfully explores the room containing the source. Once the average RSSI exceeds the threshold, the robot stops.

The average RSSI is plotted in Fig. 7 over the distance covered by the robot. We consider highlight the behavior of the algorithm as the robot explores the environment (see Fig. 6 for a helpful map). In epoch (A), the time until A in the figure, the robot observes weak RSSI while performing area exploration. The robot is able to extract gradient information to steer it down the hallway towards the source. In epoch (B), the robot observes steadily increasing gradient, thus corroborating the decision to move down the hallway. Note that though the average RSSI shows the effect of strong fading, the gradient estimate is able to detect the gradual trend of the RSSI. The robot nears the entrance to the source room by epoch (C), but in epoch (D), it continues down the hallway. However, before it makes it too far, the waypoint drops in ranking sufficiently for it to turn around and reach the goal state in epoch (E).

In order to accelerate simulations, the robot is confined to move on the grid and looks up the RSS value for each location based on the offline EMCUBE calculations. Consequently, we assume that RSS is deterministic and takes on one value at each position on the grid. It is further assumed that the robot will exactly calculate its position and the positions of obstacles. As a result, the path-distance to frontiers can always be accurately calculated and continuous evaluation of frontiers is precise. It is also assumed that the robot can explore every identified frontier so only $k = 8$ potential frontiers need to be considered for each calculation. An example of one simulation trial is depicted in Fig. 9.

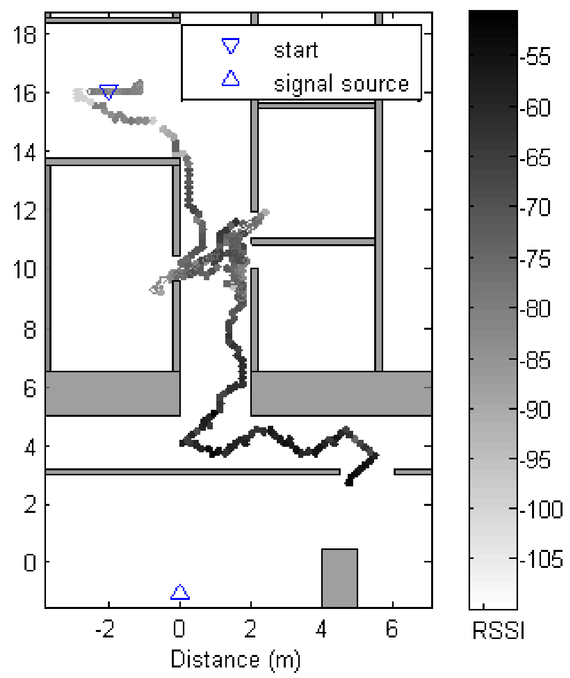

Fig. 9. Physical environment with simulated test result trajectory

The robot first explores its immediate surroundings (the upper hallway), to obtain a good RSS gradient estimate. Then it transitions to RSS frontier exploration. Its exploration leads it to sample the RSS in several rooms. Though it enters the rooms, it quickly decides to leave because the RSS gradient points back to the hallway. The controller ultimately leads the robot to the signal source in the large lower room. Once the robot observes a sufficiently high average RSS, the goal condition is reached.

In order to further examine certain parameters, several tests were performed. The first involved changing the oscillation amplitude (i.e., amount of deviation from the straight path) of the robot as it tracked waypoints. The second involved removing the gradient and RSS average components to determine their effects on efficiency/capability on the controller.

The RSS exploration algorithm has a number of variables which affect how it executes. One such value is the number of frontiers to consider. As the number of frontiers increases, calculation time increases as well. In addition, the number of frontiers should be limited such that small cleared areas are not calculated as frontiers. This variable is also strongly tied to which approach is used for the k-means portion of frontier identification. Values between 4 and 10 work well in simulation.

Finally, we examine the number of collected RSS points required to form a subset for frontier evaluation. This parameter is related to how how constricted the environment is in contrast with the distance for assumed independence of points. In a very constricted environment where points are independent at larger distances, only a few points should be averaged together. In open environment with small distances required for independence, it is advisable to average 10 to 20 RSS samples together. The parameters used for the experiments and simulations are enumerated in Table I.

A. Effect of Oscillation

We investigate how much the robot should deviate from the straight-line path as it moves towards each waypoint. Figure 10 shows the results of these tests. This plot shows the total distance traveled to reach the robots goal condition as well as how often these path distances occurred.

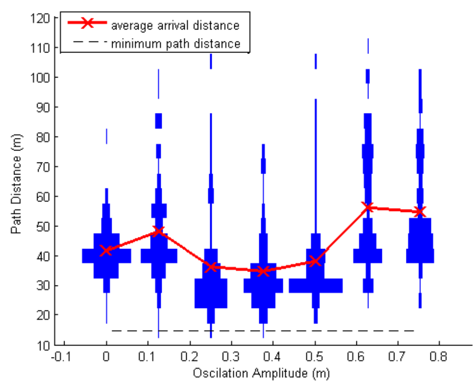

Fig. 10. Path length to source with different deformation amplitudes. This total distance frequency is depicted by sorting the values into bins. The width of each bar is directly correlated with the number of occurrences.

In this set of simulations, there is a greater concentration of shorter total path distances than longer path distances. However, the robot was able to improve its sampled RSS and move towards the source without exploring a large portion of the environment.

As the oscillation increases from 0 to 0.375 m, the average distance traveled decreases. This improvement in efficiency is due to more accurate gradient estimates from spatially separated RSS measurements (see Section II). As the oscillation increases beyond 0.375 m, we see that the improved gradient estimates become offset by the increase in distance traveled.

B. Effects of RSS Gradient and RSS Average

Determining the how the RSS gradient and average magnitude contribute to the efficiency of the control is the objective of this test. In Fig. 11, the algorithm is tested with an oscillation amplitude of 0.375 m while changing the method for choosing frontiers.

This figure show the results from three different tests with ten trials each. In the first test, the algorithm was tested using both RSS average magnitude and gradient information. In the two subsequent tests, either the gradient or the average

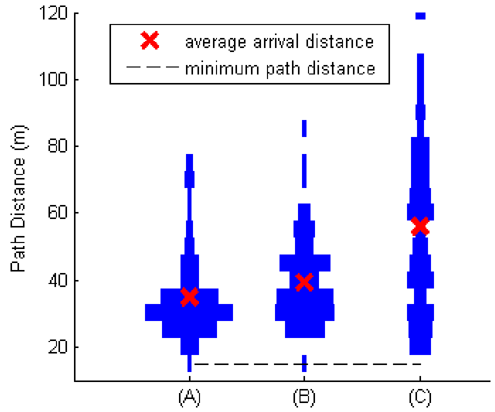

Fig. 11. (A) Test using both RSS gradient and average (B) Test using average only (C) Test using gradient only

magnitude was used along with the distance weight to choose frontiers. These results show that while it is possible to weight frontiers with only RSS average magnitude or RSS gradients, better efficiency can be obtained by using both. Both sets of tests for RSS average magnitude and gradient have similar means and standard variations.

V. Conclusions

We have developed and demonstrated a new algorithm that seeks a radio source in an indoor environment. Our approach uses RSS gradient estimation to prioritize the frontier exploration options. Several metrics for RSS spatial sampling while approaching the signal source were developed and implemented. The resulting control algorithm is applicable to a wide variety of scenarios because it does not require knowledge of the propagation environment beyond basic fading assumptions and does not require a map a priori.

Interesting directions for further study include multiple agents, and moving sources. Collaborative agents could lead to increased exploration efficiency, and these agents can also exploit RSS amongst themselves to maintain connectivity. Similarly, adapting to a moving source leads to control algorithms that can be exploited to maintain or enhance connectivity in a mobile ad hoc network (MANET).

Appendix I
RSS Gradient Estimation

We assume that a mobile sensor makes RSS measurements Z_i at locations $(X_{i,1}, X_{i,2})$ for $1 \le i \le n$. We center the locations so

$$\sum_i^n X_{i,1} = \sum_i^n X_{i,2} = 0\,. \qquad (1)$$

We are interested in finding the gradient of the RSS measurements. We perform a 2-dimensional least-squares estimation, i.e., we fit a plane to the measurements. $\mathbf{Z}$ is a random $n \times 1$ column vector and $\mathbf{X}$ is a $n \times 2$ matrix. The gradient β is a 2×1 column vector that indicates the direction of steepest gradient ascent,

$$\begin{aligned} \mathbf{X}\beta &= \mathbf{Z} && (2)\\ \beta &= (\mathbf{X}^T\mathbf{X})^{-1}\mathbf{X}^T\mathbf{Z} && (3) \end{aligned}$$

Equation (3) is the least-squares solution with 2 parameters with centered data [13]. This centering of the locations allows us to disregard any constant offset in the RSS measurements, because from (1) and (3) we see that

$$\mathbf{X}^T\mathbf{Z} = \mathbf{X}^T(\mathbf{Z} + c\mathbf{1}^{n\times 1})$$

for some scalar c.

The estimated gradient direction and slope magnitude is

$$\begin{aligned} \hat{\theta}_S &= \tan^{-1}\frac{\beta_2}{\beta_1} && (4)\\ |\beta| &= \sqrt{\beta_1^2 + \beta_2^2} && (5) \end{aligned}$$

From (3) we observe that $\mathbf{X}^T\mathbf{X}$ must be non-singular for a unique solution of β. Geometrically, the sampling locations must not be co-linear. We use singular value decomposition (SVD) to write $\mathbf{X} = \mathbf{USV^T}$ where $\mathbf{U}, \mathbf{V}$ are unitary and $\mathbf{S}$ is diagonal. We note that $\mathbf{X}^T\mathbf{X}$ is symmetric and therefore its eigenvectors (columns of $\mathbf{V}$) are orthogonal. We can then rotate the coordinate system so that the eigenvectors are $< 1, 0 >$ and $< 0, 1 >$, i.e., $\mathbf{V} = \mathbf{I}$ and so $\mathbf{X} = \mathbf{US}$.

When $\mathbf{X}^T\mathbf{X}$ is non-singular, (3) can be written

$$\begin{aligned} \beta &= (\mathbf{S}^T\mathbf{S})^{-1}(\mathbf{S}^T\mathbf{U}^T)\mathbf{Z} && (6)\\ &= \mathbf{S}^+\mathbf{U}^T\mathbf{Z} && (7)\\ &= \mathbf{X}^+\mathbf{Z} && (8) \end{aligned}$$

where $(\cdot)^+$ indicates psuedo-inverse, e.g., $\mathbf{X}^+\mathbf{X} = \mathbf{I}$. The diagonal elements of $\mathbf{S}^+$ are the inverse root eigenvalues of $\mathbf{X}^T\mathbf{X}$, i.e., $1/\sqrt{\lambda_1}, 1/\sqrt{\lambda_2}$.

Appendix II
Efficient Sampling for RSS Gradient

Successful estimation of RSS gradient requires a strategy for sampling inside a physical environment. In particular, straight-line trajectories lead to degenerate gradient estimates, as discussed in Section I. We discuss how the we perturb the paths in order to improve the accuracy of our gradient estimates.

The ranking of the frontiers relies on the accuracy of the RSS gradient estimate, which in turn depends on where the RSS measurements are taken. That is, the RSS sampling strategy strongly affects the reliability of the RSS gradient estimates β, which we quantify by its variance

$$\begin{bmatrix} \mathrm{Var}[\beta_1] \\ \mathrm{Var}[\beta_2] \end{bmatrix} = \mathbf{X}^{+2} \begin{bmatrix} \mathrm{Var}[Z_1] \\ \vdots \\ \mathrm{Var}[Z_n] \end{bmatrix} \qquad (9)$$

where we define $X_{ij}^{+2} = (X_{i,j}^+)^2$. We do not make any assumptions on the variance of the observations $\mathbf{Z}$, but instead focus on reducing the variance by modifying our sampling strategy, dictated by the sampling locations $\mathbf{X}$.

As discussed in Section I, the measurement locations should not be co-linear, otherwise the gradient calculation is degenerate.

For an idea of how the variance of the RSS gradient depends on $\mathbf{X}$, consider the situation when $\mathrm{Var}[Z_i] = \mathrm{Var}[Z]$ for $1 \leq i \leq n$. It follows from (7) and (9) that

$$\begin{bmatrix} \mathrm{Var}[\beta_1] \\ \mathrm{Var}[\beta_2] \end{bmatrix} = \begin{bmatrix} 1/\lambda_1 \\ 1/\lambda_2 \end{bmatrix} \mathrm{Var}[Z] \tag{10}$$

where λ_1, λ_2 are the eigenvalues of $\mathbf{X}^T\mathbf{X}$. Thus the variance of the gradient decreases as the eigenvalues of the locations matrix $\mathbf{X}$ increase. Geometrically, this guides us to consider sampling locations are spread further apart rather than confined to a small region.

Fig. 12 plots $(\lambda_1 + \lambda_2)/2$ for simple sampling strategies (regular polygon, square, rectangular spiral), for a fixed distance traveled. The regular polygon and square have comparatively large confidence because measurements are well separated spatially, but the spiral takes measurements in a more confined manner. We note that these strategies are approximately rotationally symmetric and thus the eigenvalues in either direction are roughly equal. Thus these strategies are well-suited for RSS gradient estimation in low-SNR regimes, where no prior gradient information is known.

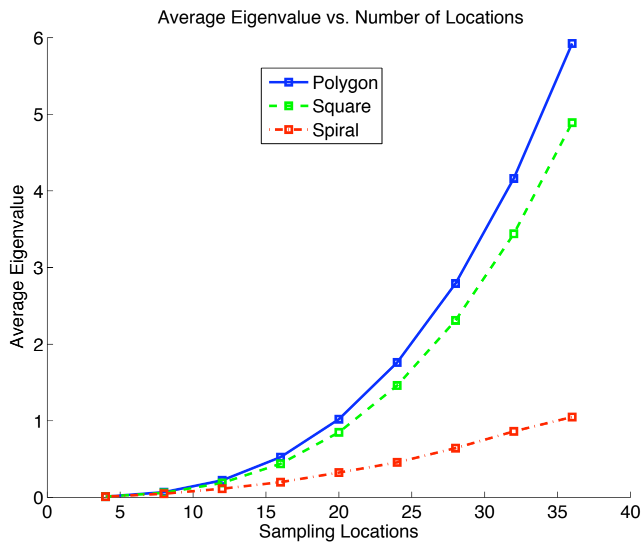

Fig. 12. Eigenvalues of simple sampling strategies

When prior gradient estimates are available, a different sampling strategy can be employed to make more efficient movements. For example, suppose that the previous gradient estimate guides the movement in direction θ. Rather than traversing a regular polygon, a zig-zag or gently oscillating path in direction θ can be taken instead (see Fig. 4). Equation (9) indicates that this directional strategy leads to high quality (lower variance) gradient estimates in the direction of travel θ, but low quality (higher variance) estimates perpendicular to θ. The disparity of the variance depends on how elongated the strategy is. If the movement is over a thin strip, confirmation of the RSS gradient will be reliable in the direction of travel, but the decision to change trajectory will be less reliable. Thus unless we are extremely confident that θ is correct, we want the sampling strategy have reasonable spatial separation in both dimensions.

REFERENCES

[1] D. Tse and P. Viswanath, *Fundamentals of Wireless Communications*. Cambridge University Press, 2005.

[2] M. A. Hsieh, A. Cowley, V. Kumar, and C. J. Taylor, "Maintaining network connectivity and performance in robot teams," *J. Field Robot.*, vol. 25, no. 1-2, pp. 111–131, 2008.

[3] Y. Mostofi, M. Malmirchegini, and A. Ghaffarkhah, "Estimation of communication signal strength in robotic networks," in *IEEE International Conference on Robotics and Automation (ICRA)*, 2010, pp. 1946 –1951.

[4] J. Fink and V. Kumar, "Online methods for radio signal mapping with mobile robots," in *IEEE International Conference on Robotics and Automation (ICRA)*, 2010, pp. 1940–1945.

[5] P. Yu, J. Twigg, and B. Sadler, "Radio signal strength tracking and control for robotic networks," in *Proceedings of SPIE*, vol. 8031, 2011, p. 803116.

[6] Y. Sun, J. Xiao, X. Li, and F. Cabrera-Mora, "Adaptive Source Localization by a Mobile Robot Using Signal Power Gradient in Sensor Networks," in *IEEE GLOBECOM 2008*, November 2008, pp. 1–5.

[7] D. Han, D. G. Andersen, M. Kaminsky, K. Papagiannaki, and S. Seshan, "Access Point Localization using Local Signal Strength Gradient," in *Passive & Active Measurement (PAM)*, Seoul, South Korea, Apr. 2009.

[8] A. Wadhwa, U. Madhow, J. Hespanha, and B. Sadler, "Following an rf trail to its source," in *49th Annual Allerton Conference*, 2011.

[9] B. Yamauchi, "A frontier-based approach for autonomous exploration," in *Computational Intelligence in Robotics and Automation, 1997. CIRA'97., Proceedings., 1997 IEEE International Symposium on*. IEEE, 1997, pp. 146–151.

[10] T. Kanungo, D. Mount, N. Netanyahu, C. Piatko, R. Silverman, and A. Wu, "An efficient-means clustering algorithm: Analysis and implementation," *IEEE Transactions on Pattern Analysis and Machine Intelligence*, pp. 881–892, 2002.

[11] M. Lindhe, K. H. Johansson, and A. Bicchi, "An experimental study of exploiting multipath fading for robot communications," in *Proceedings of Robotics: Science and Systems*, 2007.

[12] EMAGWARE, *EM.CUBE 2010 Propagation Manual*, 2010.

[13] N. Draper and H. Smith, *Applied Regression Analysis*, 3rd ed., ser. A Wiley-Interscience publication. New York, NY: Wiley, 1998.